IJE TRANSACTIONS B: Applications Vol. 37 No. 02, (February 2024) 237-251

International Journal of Engineering

Journal Homepage: www.ije.ir

A Novel Design and Simulation of a Nano Prosthetic Artificial Heart Valves

S. Mahmood Ali*

Biomedical Engineering Department, University of Technology, Iraq

PAPER INFO

Paper history:
Received 14 April 2023
Received in revised form 01 November 2023
Accepted 02 November 2023

Keywords:
Artificial Caged Ball Valve
Single-Leaflet Heart Valves
Heart Valves Simulation
Tricuspid Aortic Valve
PSN4
SIBSTAR103T

ABSTRACT

Heart valve replacement is a major health burden and is required by millions of people worldwide, which invites the continuous need to discover and manufacture more effective and permanent artificial replacements. In the present work, unique models of eight artificial heart valves were designed and examined using seven synthetic and nanocomposite materials. The designed valves were examined to determine the best designs and materials in terms of durability, flexibility, and energy consumption, and to improve the biomechanical performance by using the Response Surface Methodology (RSM) and the Design Expert System 13. The highest values of the equivalent stress due to the applied blood pressure on the moving parts on each type of manufactured heart valve occur in valves with three dimensions moving parts, reached in the mitral tri-leaflet valve 14.13 MPa, followed by the tricuspid aortic valve. The equivalent stresses for other types of valves produced with simple surface action were lower than 2 MPa. The strain energy that is expended during the process of diastole and systole was found to be directly proportional to the strength and flexibility of the materials used. The energy consumption rates decrease when using highly elastic materials such as TPE and PSN4. The values of this energy also increase with an increase in the area of the moving parts of the valve, especially when faced with the process of closing blood flow, as with the use of the tricuspid aortic valve (TAV). The highest total deformation resulted in the valve body when using TPU, followed by TPE, nylon, PETG, and PLA, while the lowest deformation rates were observed when using PSN4, which ranged from $5x10^5$ to 0.1 mm, followed by SIBSTAR103 nanostructured rubber. The obtained values of stress safety factors were decreased with the complexity of the movement for the moving parts of the valve. The highest rates were recorded when using the tricuspid mitral valve, reaching 2.45 when using the high-strength and flexible PSN4 nanomaterial. It can be concluded that the best materials for manufacturing these four types of valves are the PSN4, followed by SIBSTAR103T, TPU, and TPE. The use of PETG, PLA, and nylon materials is not recommended for the manufacture of any prosthetic heart valves, due to their lack of strength, flexibility, and high brittleness, especially for PETG and PLA materials. It was also noted here that PSN4 is the only material suitable for the manufacture of mitral tri-leaflet and tricuspid mitral valve artificial valves. For other types of valves manufactured with a single leaflet, high safety stress factors were obtained because their movement is simple, flat, and in one direction, where the highest values were observed when testing a single hemispherical leaflet type valve, then the conical caged ball and the caged ball type, respectively.

***doi**: 10.5829/ije.2024.37.02b.03*

Graphical Abstract

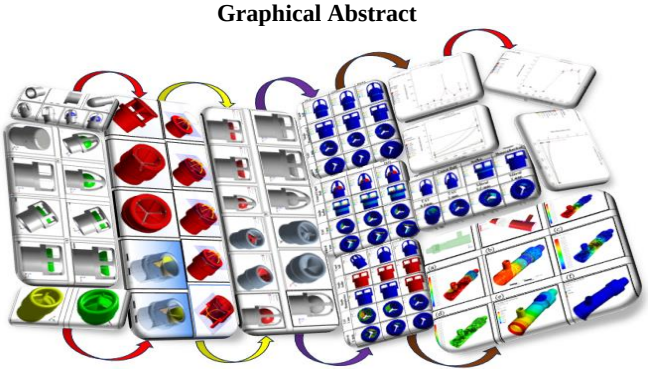

*Corresponding author email: *30249@uotechnology.edu.iq* (S. Mahmood Ali)

Please cite this article as: Mahmood Ali S. A Novel Design and Simulation of a Nano Prosthetic Artificial Heart Valves. International Journal of Engineering, Transactions B: Applications. 2024;37(02):237-51.

NOMENCLATURE

CFD	Computational Fluid Dynamics	a	Dimensionless parameters; a = δ/R0
FVM	Finite volume method	b	Dimensionless parameters; $b = (m/L_0)^2$
PETG	Polyethylene Terephthalate Glycol	k	The flow consistency index
PLA	Polylactic Acid	L	The half-length of an artery model (cm)
PSN4	Polyetherimide/Silicone Rubber	L_0	half-length of the artery stenosis(cm)
RSM	Response Surface Methodology	m	Constant value
SIBSTAR103T	Isobutylene-B-Styrene Rubber Triblock	n	The power-law index
TAV	Tricuspid Aortic Valve	p	The blood pressure (mmHg)
TPE	Thermoplastic Polyurethane Elastomer	Q	Blood flow rate (liter/min.)
TPU	Thermoplastic Polyurethane	Q_0	Initial value of blood flow rate (cm^3/sec)
VHD	Valvular Heart Disease	r	Radial coordinate transformation, r = yR,
τ_{rz}, τ_{rr}, *and* τ_{zz}	The shear stresses of the model	$R(z)$	The a stenosed artery's radius (mm)
τ_{ij}	The Reynolds stress	R_0	The radius of a normal artery (cm)
ρ	Blood density (kg/m^3)	Re	Reynolds number
λ	The resistance to the blood flow	S	Modulus of the mean rate-of-strain
μ	Dynamic viscosity of blood (Pa s)	S_0	Initial blood vessel cross-sectional area (cm^3)
δ_{ij}	Parameter controls the percentage stenosis.	V	The bulk stream-wise velocity related Re
δ	The highest depth of the stenosis (cm)	Vr	The blood radial velocity
v	The blood parabolic velocity profile (m/s)		

1. INTRODUCTION

Congenital and rheumatic valvular heart disease (VHD) is the most important cause of heart failure around the world (1-3), which can cause arrhythmias, stroke, heart failure, and potentially life-threatening complications and need continuous clinical attention. More than 30 million people suffer from it. In the United States alone, approximately 90,000 heart valve replacements and more than 300,000 worldwide are performed annually with biomechanical or prosthetic valves (4).

Each human heart has four valves: the mitral, the tricuspid, the aortic, and the pulmonary valve (1, 5). There are various forms of aortic valve disease, namely aortic regurgitation, aortic stenosis, congenital aortic valve disease, and atrial septal defect (6). Artificial heart valves are used to replace heart valves that have been damaged by disease or wear and tear for time duration (7).

Mechanical heart valves are made of materials of much higher strength than those found in human soft tissues. There are basic types of mechanical heart valve designs including, the gaged ball, single leaflet, bicuspid, and tricuspid valves (8). The main advantages of the mechanical valve are their durability, and they are well-suited for patients of all ages. These Artificial heart valves rarely need replacement and often last for the rest of the patient's life. The main drawback of a mechanical valve is its tendency to form blood clots on its surfaces, so patients need lifelong blood-thinning medications and lifestyle modifications (9).

The use of prosthetic artificial heart valves and continuous improvements in valve designs have reduced the death rate of heart patients (9). The selection of a prosthetic valve that is appropriate in shape and size is a key factor for the success of surgery (10). However, the ability of the valve geometry to provide adequate mechanical function immediately after implantation is critical to patient survival. Therefore, the successful application of tissue engineering in the development of heart valves will require that they maintain similar mechanical properties to that of the original valves, and the ability to repair, remodel, and regenerate heart tissue (11, 12). So far, no satisfactory mechanism has been found to achieve a dynamically stable and durable implantable heart valve (13). The latest designs of mechanical heart valves provide relatively superior hemodynamics, but high-shear platelets and blood cells still pose significant challenges (14).

Composite materials are one of the most well-known materials for various functions that reduce the structure's weight without reducing its strength. Polymer composites exploit a wide range of applications due to their excellent performance in mechanical, electrical, and thermal properties (such as medical, electronic, automobile, and aerospace) (15).

The current work aims to design and simulate a unique model of eight artificial heart valves using seven synthetic and nanocomposite materials. The designed valves will be examined to determine the best designs and materials in terms of durability, flexibility, and energy consumption performances by using the Response Surface Methodology (RSM) and Expert Design 13 system.

2. MATERIALS METHODOLOGY

2. 1. Design of a Human Artificial Heart Valves

The mechanical prosthetic heart valves are an effective

engineering device used to replace the damaged or diseased natural valves of the heart and are characterized by long performance and high reliability, but they may lead to possible complications such as hemolysis and thrombosis (16). Durability is the most important factor in choosing the right materials for polymeric heart valves to ensure strong mechanical properties that give the valve low creep, high rigidity with self-healing, and the ability to maintain structural integrity at repeated periodic loading and unloading of blood to prevent life-long blood clotting, and it is less prone to calcification and failure compared to bio-prosthetic valves (5).

The most important factors that must be considered when choosing a valve are the patient's age, comorbidities, and life expectancy (8). The process of designing an artificial heart valve needs to evaluate its mechanical performance and blood flow pattern and study both leaflet deformation/stress. As the leaflet is subjected to fluctuating stress, the large lifetime of the stress requires flexibility to open and close the blood flow path as a major function of the heart valve (17). The most important design requirements for valves are those that cause minimal shock to the elements of the structure surrounding the valve, blood vessels, and endothelial tissues of the heart, with good resistance to mechanical and structural abrasion. It works to reduce the chances of deposition of platelets and thrombus, to be non-dissolving materials, to be stable and not absorb blood components, and to be sterilizable with high surface quality (18).

In this work, eight artificial heart valves were designed and analyzed. Table 1 lists the main physical and mechanical properties of the designed materials.

Figure 1 illustrates the designing steps for the artificial caged ball heart prosthetic valve. The caged ball valve is the first artificial heart valve designed and implanted in the human body. The valve was initially made of stainless steel (12). The introduction of granulated ball valves is a major advance in the treatment of patients.

Now, there are several thousand patients who have such valves implanted (8, 19). The caged ball valve design is still the valve of choice for some surgeons (18, 20). It consists of a celestial ball with a circular stitching ring and a cage of three or four plastic or metal brackets (usually of titanium rods) that determines the path of movement of the ball (21).

The ball blocks the valve opening to prevent the reverse flow of blood. Its diameter is greater than the inner diameter of a circular ring.

TABLE 1. The main physical and mechanical properties of the designed materials (12, 22-29)

Filament materials	Density (g/cm^3)	Nozzle temp. (°C)	Heated bed temp. (°C)	Printing speed (mm/s)	Tensile Strength (MPa)	Tensile Elongation (%)	Impact Strength (kJ/m^2)	Flexural Strength (MPa)	Flexural Modulus (GPa)
Nylon (White)	1.16	240	85	35	6.37	231.30	28.30	8.34	0.20
PETG (Blue)	1.27	240	75	50	4.90	120.00	8.70	70.61	2.15
(TPU) Transparent (purple, orange, and yellow)	1.21	235	60	40 – 60	16.80	550.00	34.40	1.80	0.08
TPE (Red)	1.14	235	30	20-40	14.00	990.00	-	80.00	1.00
PLA (White and, Transparent purple)	1.24	200	40	50	6.08	4.40	4.20	6.47	2.75
SIBSTAR 103T	0.92	-	-	-	18.10	506.00	-	-	5.92
PSN4	1.27	-	--	-	39.13	108.50	102.60	73.24	2.43

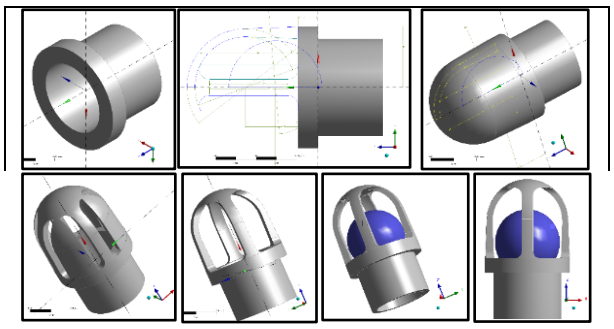

Figure 1. The designed steps of the artificial caged ball mechanical heart valve

These valves were designed to allow blood to flow in only one direction, and act to cause blood to flow from the heart to the aorta when the pressure of the heart exerts on the blood (and the valve ball) exceeds the pressure in the aorta. After the blood leaves the heart, the pressure inside the heart drops drastically, then the negative pressure sucks the ball of the valve back, which will prevent the blood from returning to the heart.

Figure 2a shows the artificial conical caged ball heart valve. This valve works with the same principle as the previous valve, except that the cage that holds the ball takes a conical shape instead of a cylindrical one to

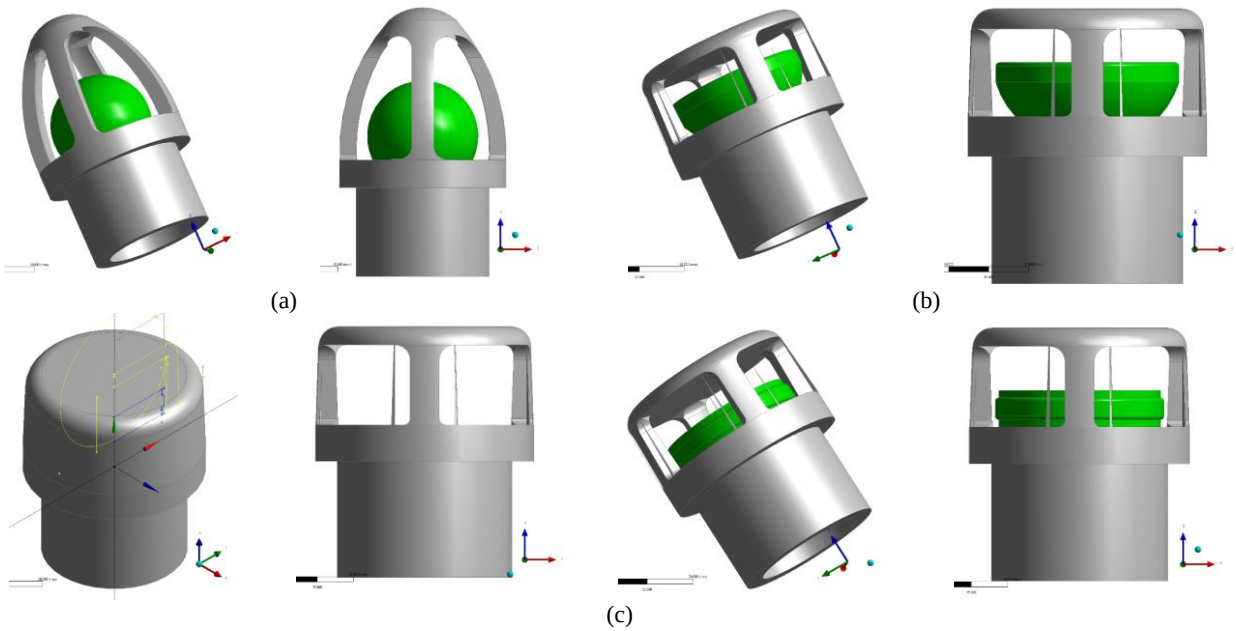

Figure 2. The designed prosthetic artificial mechanical heart valve; (a) the designed conical caged ball valve; (b); the single hemispherical caged ball valve (c) the single-leaflet valve

increase control over the alignment of the central movement of the ball when the blood is flowing or when the valve is closed.

Figure 2b shows the designed single hemispherical caged ball artificial valve, Which works in the same way as the single-leaflet disc valve, but with better peripheral blood flow dynamics, ease, and rapid closing of the valve when the blood flow stops. Figure 2c shows the designed artificial single-leaflet prosthetic valve.

It consists of four perpendicular metallic or polymeric stents to hold a disc inward above the orifice for blood flow from the heart, and the opening angle of the disc concerning the valve ring ranges from 60 to 80 degrees. This type may show a complex dynamic flow, where the kinetic energy of the blood flow must first move the disc and then centralize the circumferential flow direction around it (8). These valves are similar to caged ball valves, except that the valve shutter is a disc (22-29). This valve allows a reduction in the annulus dimensions. The thickness of the disc valve ring is about 0.13D and thus its total length is reduced to 0.82D. It works rapidly and smoothly in the velocity field in the aorta (30).

The single-disc valve has been shown to operate at a much lower rate of clots than the bileaflet valve, and the open rate is greater (31). The structures of the pulmonary and aortic valves are similar, and both are made of three semilunar leaflets within the valve roots (5). Following the great success of interest treatments have grown in treatments to include the mitral valve. The first therapeutic mitral valve implanted in humans was approved by the Food and Drug Administration in 2013. Since then, several technologies have been developed and are currently being investigated (32). The structures of the pulmonary and aortic valves are similar, and both are made of three semilunar leaflets within the valve roots (5).

Figure 3 shows the designing steps of an artificial mitral tri-leaflet heart valve. This valve has been designed to work on the same principles as the previous valve, except that it allows the oxygen-rich blood to flow from the heart into the aorta. The prototype of this valve was produced from a short silicone rubber tube and a metal ring (33).

Then the design was improved by making it without a metal ring.Tricuspid valve disease is an unmet clinical need. Tricuspid valve disease is a common valvular with high patient and mortality rates. Yet tricuspid valve surgery remains the most dangerous of all valvular surgeries with an estimated inpatient mortality rate of 8.8%.

Due to the novelty of these techniques and the complex and variable anatomy of the tricuspid valve, procedural planning, and research based on 3D printing are of great value (32). Increased interest in tricuspid valve replacement has led to the advancement of 3D printing models of this valve (34-36). Tricuspid polymeric valves were developed that better resemble the original valve geometries and are more dynamically efficient. Figure 4 shows the designed tricuspid prosthetic aortic valve (TAV). It consists of three leaflets of equal shape and size (37).

This valve allows blood to flow from the aorta into the heart. It is a replacement for the bicuspid aortic valve which is a congenital defect since it is not able to completely stop the blood from leaking back into the heart. This can harden and not-open the valve, causing the heart to pump harder to bypass the aortic valve stenosis.

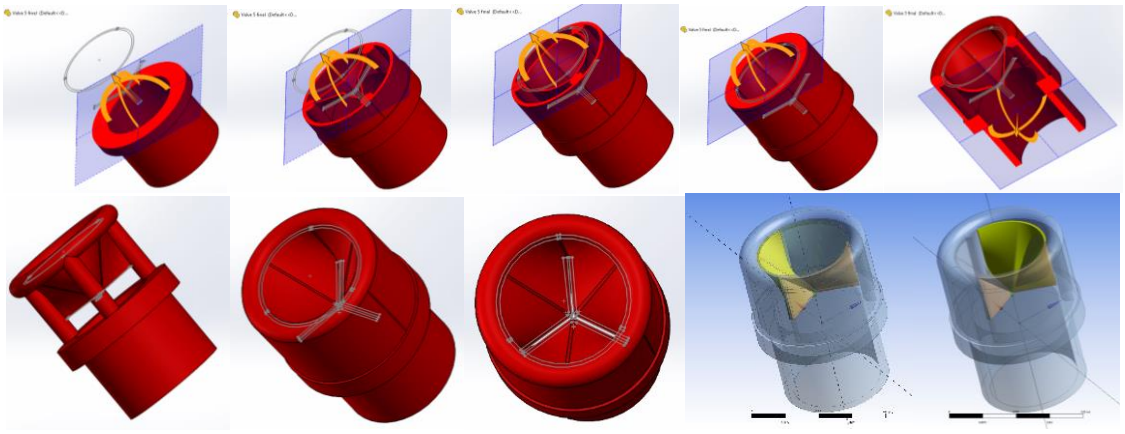

Figure 3. The designing steps mitral tri-leaflet heart artificial valve

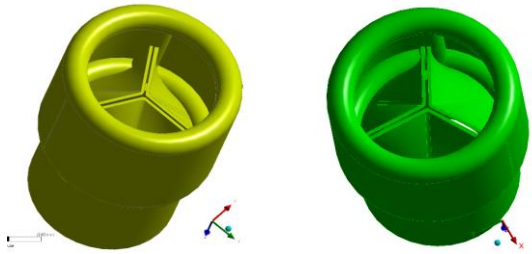

Figure 4. The designed tricuspid prosthetic aortic valve (TAV)

2. ٢. Mathematical Modeling of the Blood Flow

The blood in the human body contains liquid and solid parts. The liquid part of the blood is called plasma, generally made of water, protein, and salts, and over 50% of blood is plasma. For developing the Cardiovascular system equation, the artery material is assumed to be non-deformable, isotropic, tapered, without longitudinal movements, and incompressible with circular sections (38). To derive the equations governing the blood fluid flow, let us assume that the blood fluid flow is assumed to be axisymmetric and incompressible (39). However, under conditions of high blood flow, particularly in the ascending aorta, the laminar flow can be turbulent and disrupted and can be described as chaotic. Turbulence flow generates heat and is dissipated, as the increases the energy required to drive blood flow because turbulence increases the loss of energy as friction. Turbulence occurs when the velocity of flow becomes high enough that the flow lamina separates and when a critical Reynolds number (Re) is exceeded. Reynolds number is a way to predict, under ideal conditions, when turbulence will occur (40).

It's important to recognize that the Navier-Stokes equations are used based on the assumption of Newtonian fluid behavior, where the viscosity is constant regardless of the shear rate. However, in microcirculatory systems such as small branches and capillaries or regions with disturbed flow patterns like the blood flow through the mechanical artificial heart valves, blood exhibits non-Newtonian flow patterns as treated in the current work (39). The equations that describe the geometry of the artificial heart stenosis models in a bell shape can be expressed as in Equation 1:

$$R(z) = -R_0\left(1 - ae^{-b(z-L)^2}\right) \quad (1)$$

where a and b are the dimensionless parameters; a = δ/R0 is the ratio of stenosed depth = 0.03–0.08 cm and the radius of a normal artery and b =(m/L0)2 is the square of the ratio of constant value m =1.4–1.8, and the half-length of the stenosis. Let the common parameters such as the radius of a normal artery (R0); R(z) is the radius of a stenosed artery; (L0) is the half-length of the stenosis; (L) is the half-length of an artery, and δ is the highest depth of the stenosis.

The blood flow model in an arterial segment is considered to be steady, incompressible, laminar, axisymmetric, and two-dimensional. The Boussinesq approximation is used to approximate the turbulent stresses existing by the turbulent dynamic viscosity (41). Then neglecting the orientation of gravity inside the body, the continuity and momentum equations for a non-Newtonian behavior, for the current blood flow study through the heart valve stenosis when the shear rate is less than 100 s-1. The equation of continuity can be written in the cylindrical coordinates system (r, θ, z) as follows (39, 42, 43):

$$\frac{\partial v_r}{\partial r} + \frac{v_r}{r} + \frac{\partial v_z}{\partial z} = 0. \quad (2)$$

The equation of momentum is:

$$v_r \frac{\partial v_z}{\partial r} + v_z \frac{\partial v_z}{\partial z} = -\frac{1}{p}\frac{\partial p}{\partial z} - \frac{1}{\rho}\left(\frac{1}{r}\frac{\partial (r\tau_{rz})}{\partial r} + \frac{\partial \tau_{zz}}{\partial z}\right) \quad (3)$$

$$v_r \frac{\partial v_r}{\partial r} + v_z \frac{\partial v_r}{\partial z} = -\frac{1}{p}\frac{\partial p}{\partial r} - \frac{1}{\rho}\left(\frac{1}{r}\frac{\partial (r\tau_{rr})}{\partial r} + \frac{\partial \tau_{rz}}{\partial z}\right) \quad (4)$$

where, τrz, τrr, and τzz are the shear stress of the model; vz is the axial velocity, p is the pressure of the fluid, vr is the radial velocity, and ρ is the density of the fluid, and:

$$\tau_{rz} = -k\gamma^{n-1}\left(\frac{\partial v_r}{\partial z} + \frac{\partial v_z}{\partial r}\right) \quad (5)$$

$$\tau_{zz} = -2k\gamma^{n-1}\left(\frac{\partial v_z}{\partial z}\right) \quad (6)$$

$$\tau_{rr} = -2k\gamma^{n-1}\left(\frac{\partial v_r}{\partial r}\right) \quad (7)$$

where k is the flow consistency index = 0.02 and:

$$\gamma = \sqrt{2\left[(\frac{\partial v_r}{\partial y})^2 + (\frac{v_r}{r})^2 + (\frac{\partial v_z}{\partial z})^2\right] + (\frac{\partial v_r}{\partial z} + \frac{\partial v_r}{\partial r})^2} \quad (8)$$

On the arterial wall, the axial velocity gradient is assumed to be zero, which means there is no shear rate of blood fluid along the axis and also there is no radial flow along the axis of the artery. Then the boundary conditions can be expressed as follow:

$$v_r(r,z) = 0, \quad \frac{\partial v_z}{\partial r}(r,z) = 0, \quad \tau_{rz} = 0, \quad on\ r = 0, \quad (9)$$

$$v_r(r,z) = 0, \quad v_z(r,z) = 0, \quad on\ r = R(z). \quad (10)$$

To immobilize the arterial wall, the radial coordinate transformation of governing equations can be used, where y=r/R(z). Then Equations 2 to 7 can be written as follow:

$$\frac{1}{R}\frac{\partial v_r}{\partial y} + \frac{v_r}{yR} + \frac{\partial v_z}{\partial z} - \frac{y}{R}\frac{dR}{dz}\frac{\partial v_z}{\partial y} = 0, \quad (11)$$

$$\left[-\frac{v_r}{R} + v_z\frac{y}{R}\frac{dR}{dz}\right]\frac{\partial v_z}{\partial y} - v_z\frac{\partial v_z}{\partial z} - \frac{1}{\rho}\frac{\partial p}{\partial z} - \frac{1}{\rho}\left[\frac{\tau_{yz}}{yR} + \frac{1}{R}\frac{\partial \tau_{yz}}{\partial z} - \frac{y}{R}\frac{dR}{dz}\frac{\partial \tau_{yz}}{\partial y}\right] = 0, \quad (12)$$

$$\tau_{yz} = -k\gamma^{n-1}\left(\frac{\partial v_r}{\partial z} - \frac{y}{R}\frac{dR}{dz}\frac{\partial v_r}{\partial y} + \frac{1}{R}\frac{\partial v_z}{\partial y}\right) \quad (13)$$

$$\tau_{zz} = -2k\gamma^{n-1}\left(\frac{\partial v_z}{\partial z} - \frac{y}{R}\frac{dR}{dz}\frac{\partial vz}{\partial y}\right), \quad (14)$$

where,

$$\gamma = \sqrt{2\left[(\frac{1}{R}\frac{\partial v_r}{\partial y})^2 + (\frac{v_r}{yR})^2 + (\frac{\partial v_z}{\partial z} - \frac{y}{R}\frac{dR}{dz}\frac{\partial v_z}{\partial y})^2\right] + (\frac{\partial v_r}{\partial z} - \frac{y}{R}\frac{dR}{dz}\frac{\partial v_r}{\partial y} + \frac{1}{R}\frac{\partial v_z}{\partial y})^2}. \quad (15)$$

The transformation initial and boundary conditions are (43):

$$v_r(y,z) = 0, \quad \frac{\partial v_z}{\partial y}(r,z) = 0, \quad \tau_{yz} = 0, \quad on\ y = 0, \quad (16)$$

$$v_r(y,z) = 0, \quad v_z(y,z) = 0, \quad on\ y = 1. \quad (17)$$

The radial velocity can be solved by multiplication of yR in Equation 11 and then integrated concerning y from 0 to 1, then:

$$\left[v_r\right]_0^1 = \left[y\frac{dR}{dz}v_z\right]_0^1 - \frac{R}{y}\int_0^1 y\frac{\partial v_z}{\partial z}dy - \frac{2}{y}\frac{dR}{dz}\int_0^1 yv_z dy. \quad (18)$$

By using the boundary condition (of Equation 16), Equation 18 will take the form:

$$\int_0^1 y\frac{\partial v_z}{\partial z}dy = -\frac{2}{R}\frac{dR}{dz}\int_0^1 yv_z dy. \quad (19)$$

Since R = R(z), Equation 19 can be re-written as:

$$\int_0^1 y\frac{\partial v_z}{\partial z}dy = -\int_0^1 y\frac{2}{R}\frac{dR}{dz}v_z dy. \quad (20)$$

By comparing both sides of the Equation 20, will give:

$$\frac{\partial v_z}{\partial z} = -\frac{2}{R}\frac{dR}{dz}v_z. \quad (21)$$

Substituting Equation 21 into Equation 11 and multiplying by yR, then:

$$y\frac{\partial v_r}{\partial y} + v_r = 2y\frac{dR}{dz}v_z + y^2\frac{dR}{dz}\frac{\partial v_z}{\partial y}. \quad (22)$$

Equation 22 can be re-written as follows:

$$\frac{\partial v}{\partial y}(yv_r) = \frac{\partial}{\partial y}\left(y^2\frac{dR}{dz}v_z\right). \quad (23)$$

Finally, the radial velocity is obtained with the form:

$$v_r = y\frac{dR}{dz}v_z. \quad (24)$$

To obtain the blood radial velocity (vr), it is required to plug vr in Equation 12, then equations of axial momentum can be reduced to:

$$-v_z\frac{\partial v_z}{\partial z} - \frac{1}{\rho}\frac{\partial p}{\partial z} - \frac{1}{\rho}\left[\frac{\tau_{yz}}{yR} + \frac{1}{R}\frac{\partial \tau_{yz}}{\partial y} + \frac{\partial \tau_{zz}}{\partial z} - \frac{y}{R}\frac{dR}{dz}\frac{\partial \tau_{yz}}{\partial y}\right] = 0. \quad (25)$$

The volumetric blood flow rate (Q) is given by the following equation:

$$Q = \int_0^R\int_0^{2\pi} v_z r\,d\theta dr = 2\pi\int_0^R v_r r\,dr. \quad (26)$$

And, using the radial coordinate transformation, r = yR, then:

$$Q = 2\pi R^2\int_0^1 v_r y\,dy. \quad (27)$$

Then, the radial velocity can be solved by discretization of Equation 24 as follows:

$$(v_r)_{i.j} = y_i\left(\frac{dR}{dz}\right)_j(v_z)_{i.j} \quad (28)$$

The volumetric flow rate can be approximated by discretizing Equation 27:

$$Q_j = 2\pi R_j^2 \Delta y \sum_{i=1}^{N+1} (v_z)_{i,j}\, y_i \quad for\ j = 1,2,...,M+1 \tag{29}$$

The resistance to the blood flow (λ) can be obtained as:

$$\lambda_j = \frac{\Delta p}{Q_j}. \tag{30}$$

To develop the mathematical model of blood pressure, Poiseuille's equation is considered to determine the relation between blood flow rate and pressure which is:

$$Q = \frac{\pi R^2}{8L\nu_z} P \tag{31}$$

Equation 25 is the mathematical model of the blood pressure in the human body. The required boundary condition and the values of the other parameters to solve these equations are; the pressure gradient, ∂ P /∂z = 40-100 mmHg, the Initial blood flow rate value of Q = 1 to 5.4 liter/minute, the Kinematic viscosity of blood, v = 0.035 cm^2/s and the density of blood ρ = 1.043 to 1.057 g/cm^3, the radius of a normal artery R0 = 0.1 cm, the constant dynamic viscosity (μ) of 3.71×10-3 Pa s, the blood density, initial value of S0 = 2.0 to 3.0 cm^3, and Q0 = 16.7 cm^3/s. For simplicity, the length of the artery model L = 14 cm, L0 = 3-8 cm, The mean Reynold number = 300, the artery systole duration for 0.3 seconds and diastole 0.5 seconds, and the period is 0.2 seconds (40, 44-46). Reynolds number and Re = of the blood flow is: Re = V * D * ρ/ μ .

۳. RESULTS AND DISCUSSIONS

The equation of the mathematical model of blood flow rate can be solved using the Computational fluid dynamics (CFD) which is a branch of fluid mechanics that uses numerical analysis system, while the finite volume method (FVM) was used for discretization of flow governing equations.

Some general settings were set for the CFD analysis in the navigation pane to perform mesh-related activities including setting up the models for the CFD simulation's viscosity by activating a multiphase and viscose model; enabling the volume and viscosity of the fluid as laminar; and enabling the Energy Equation option from the Model list, the k-epsilon and K-equation turbulence model to expand the Viscous Model (45). In CFD analysis system, the Y+ value represents the distance from the first grid cell to the surface wall is an important parameter for determining the accuracy of the boundary layer thickness (46-48).

Figure 5 represents CFD solution and simulation of the of blood flow in the atria with a tricuspid mitral valve (1mm), using the high-strength and flexible PSN4 nanomaterial.

To determine the mechanical properties of the designed artificial valves, the response surface method (RSM), the finite element method (FEM) and the Design-Expert 13 were applied (49, 50). They were first modeled with the static structures analysis system. Then the meshing process was carried out with the additional refinement fragmentation for the moving parts of the valves, which are exposed to variable loads, as shown in Figure 6a.

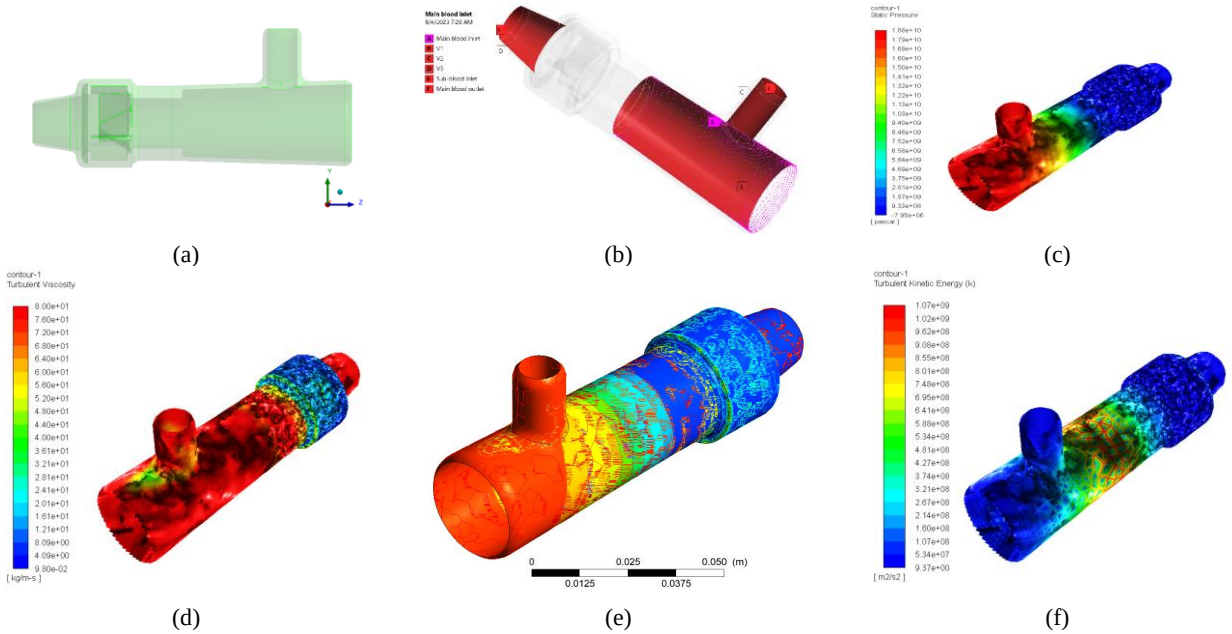

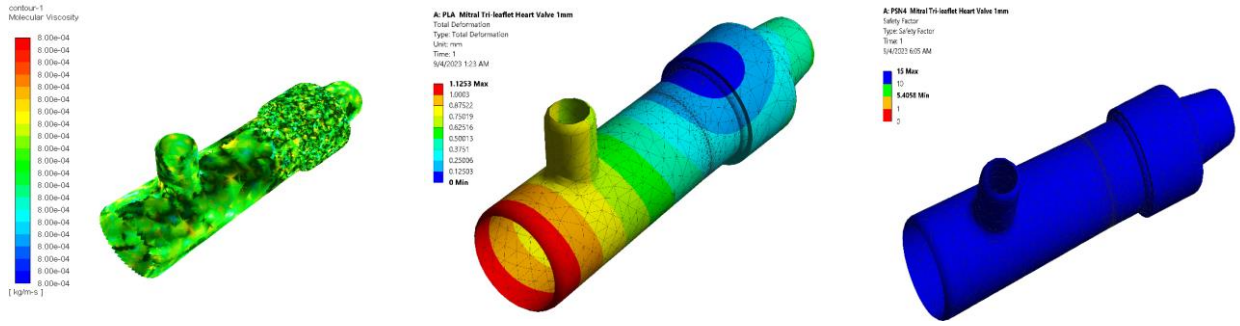

(g) (h) (i)

Figure 5. Simulation of blood flow in the atria; (a) The initial state of the artery; (b) Boundary Conditions; (c) Static pressure; (d);Turbulent viscosity (e) Eddy viscosity; (f); Turbulent kinetic energy (g) Molecular viscosity; (h) Total deformation; (i) Stress safety factor

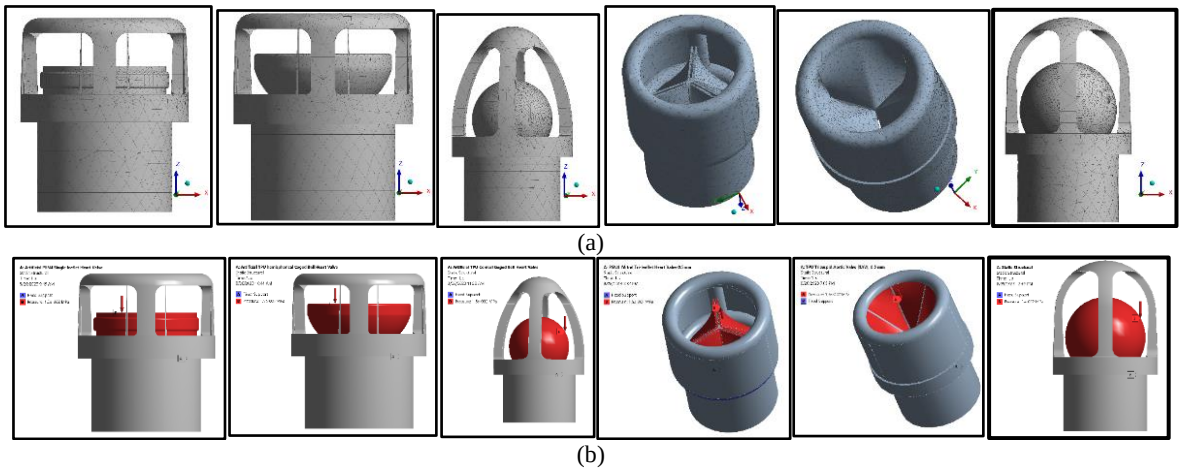

(a)

(b)

Figure 6. Modeling of the designed artificial valves; (a) The meshing process; (b) The determined boundary conditions for the applied heart blood pressure from the hear

The structure mesh has been used for gridding of each designed artificial heart valve with the number of different cells and the mesh study performed according to the required number of cells were created for gridding (51).

Then the boundary conditions for each valve were determined, where a pressure equal to the blood flowing pressure from the heart, which is mmHg, was subjected on the surface of the valve moving parts, while the base area in the assembly completion with the heart was simply supported, as shown in the Figure 6b. Table 2 illustrates the mechanical properties of the designed artificial heart valves.

Figure 7 shows The strain energy simulations for selected types and the used materials of the designed artificial heart valves. Figures 8 to 10 show the simulations models of the strain energies, the total deformations, the equivalent stresses, the stress safety factor for selected types, and the used materials of the designed artificial heart valves.

To simulate of diastolic and systolic of the natural heart at each pulse cycle, the Goodman loading ratio criteria was used for the transient continuously and repeated applied blood pressure of +200 Pa for 0.5 second followed by an absorption pressure -50 Pa for the duration for 0.3 second (47). To analyze the results, the statistical Expert Systems 13.0 program was used.

Figure 11 shows the equivalent stress values resulting and calculated from applying blood pressure on the moving parts of these valves of each type of manufactured heart valve by using the Von Mises method.

From the figure, it is clear that the highest values of the equivalent stresses were found in valves with moving parts in a large range and three dimensions.

The highest values were produced in the mitral tri-leaflet valve (tri-leaflet Thick. = 0.5 mm) reached 14.13 MPa, followed by the tricuspid Aortic valve (TAV), (tricuspid thick. = 0.5 mm and 1 mm, respectively), while the equivalent stresses for the other types of the produced valves with the simple surface movement were less than 2 MPa, and the lowest value of stress was produced in the single-leaflet type valve, which reached 0.87 MPa.

TABLE 2. The fatigue properties of the designed artificial heart valves

Artificial Heart Valve Type	Filament Material	Strain Energy (10-5 mJ)	Total Deformation (mm)	Equivalent stress (MPa)	Stress safety factor (Min.)	Artificial Heart Valve Type	Filament Material	Strain Energy (10-5 mJ)	Total Deformation (mm)	Equivalent stress (MPa)	Stress safety factor (Min.)
Caged Ball	PETG	1.866	0.001	1.499	1.601	**Tricuspid Aortic Valve (TAV), (Tricuspid Thick. = 0.5 mm)**	PETG	178.100	0.585	11.077	0.217
	PLA	1.460	0.001		1.801		PLA	139.250	0.457		0.244
	Nylon	20.553	0.015		2.001		Nylon	1960.900	6.441		0.271
	TPE	3.347	0.025		4.700		TPE	382.370	1.256		0.632
	TPU	4.008	0.032		5.337		TPU	4858.600	9.959		0.722
	SIBSTAR 103T	0.677	0.001		5.671		SIBSTAR 103T	64.589	0.212		0.767
	PSN4	0.300	0.0002		12.00		PSN4	28.642	0.094		1.625
Conical Caged Ball	PETG	0.834	0.0010	1.618	1.484	**Tricuspid Aortic Valve (TAV), (Tricuspid Thick. =1.0 mm)**	PETG	11.281	20.841	13.028	0.184
	PLA	0.649	0.0008		1.669		PLA	8.824	0.124		0.207
	Nylon	9.192	0.0113		1.855		Nylon	124.26	1.745		0.230
	TPE	1.792	0.0022		4.328		TPE	24.231	0.340		0.480
	TPU	1.792	0.0280		4.946		TPU	307.890	43.247		0.614
	SIBSTAR 103T	0.303	0.0004		5.26		SIBSTAR 103T	4.093	0.058		0.652
	PSN4	0.134	0.0002		11.12		PSN4	1.815	0.026		1.382
Single-leaflet	PETG	20.405	0.0003	0.150	15	**Mitral Tri-leaflet Valve (Tri-leaflet Thick. = 0.5 mm)**	PETG	84.590	0.629	14.132	0.170
	PLA	18.816	0.0003		15		PLA	66.168	0.492		0.191
	Nylon	2.650	0.0037		15		Nylon	931.790	6.926		0.212
	TPE	51.650	0.0007		15		TPE	181.700	1.351		0.495
	TPU	6.565	0.0090		15		TPU	2308.700	11.160		0.566
	SIBSTAR 103T	872.780	0.0001		15		SIBSTAR 103T	30.692	0.228		0.602
	PSN4	387.080	0.00005		15		PSN4	13.610	0.101		1.274
Single Hemispherical Leaflet	PETG	0.845	0.0010	0.870	2.759	**Mitral Tri-leaflet Valve (Tri-leaflet Thick. = 1.0 mm)**	PETG	62.986	0.108	7.339	0.327
	PLA	0.661	0.0008		3.103		PLA	49.269	0.085		0.368
	Nylon	9.312	0.0113		3.448		Nylon	693.810	1.194		0.409
	TPE	1.816	0.0022		8.046		TPE	135.290	0.233		0.954
	TPU	23.044	0.0280		9.195		TPU	1719.100	2.959		1.090
	SIBSTAR 103T	0.308	0.0004		9.77		SIBSTAR 103T	22.854	0.039		1.158
	PSN4	0.136	0.0002		15		PSN4	10.134	0.0170		2.453

Figure 12 shows the relationship between the produced artificial heart valve type and the filament material with the strain energy expended when blood pressures of 120 mmHg are applied on the moving parts of the manufactured heart valves from the heart to the arteries or from the veins to the heart to open or close the blood flow during the process of diastole and contraction of the heart.

This figure shows that the energy expended is directly proportional to the strength and flexibility of the used material, and the energy expenditure rates decrease when using highly flexible materials such as TPE and PSN4. The values of this energy also increase when the area of the moving parts of the valve increases, especially when the closure process is facing the blood flow, as is the case with the use of a tricuspid Aortic valve (TAV), (tricuspid thick. = 0.5 mm and 1 mm, respectively). The amount of energy increased when using the mitral tri-leaflet valve (tri-leaflet Thick. = 0.5 mm and 1 mm, respectively). The least energy was spent when using simple movement

valves in one direction, which are the conical caged ball, the single hemispherical leaflet, the caged ball, and then the single leaflet valves, respectively. In general, the highest calculated strain energy does not exceed 0.049 mJ.

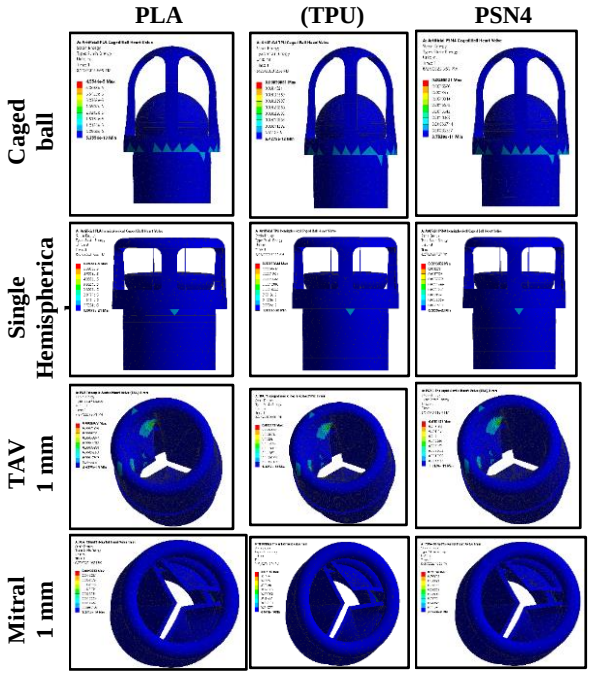

Figure 7. The strain energy simulations for selected types and the used materials of the designed artificial heart valves

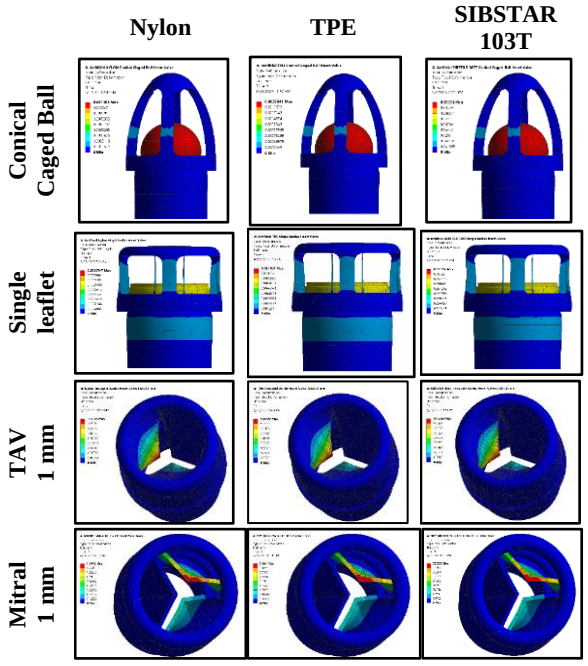

Figure 8. The total deformation simulations selected types and the used materials of the designed artificial heart valves

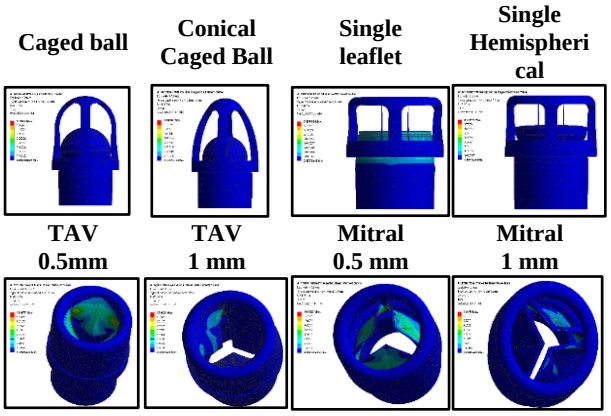

Figure 9. The equivalent stress for all the types and the used materials of the designed artificial heart valves

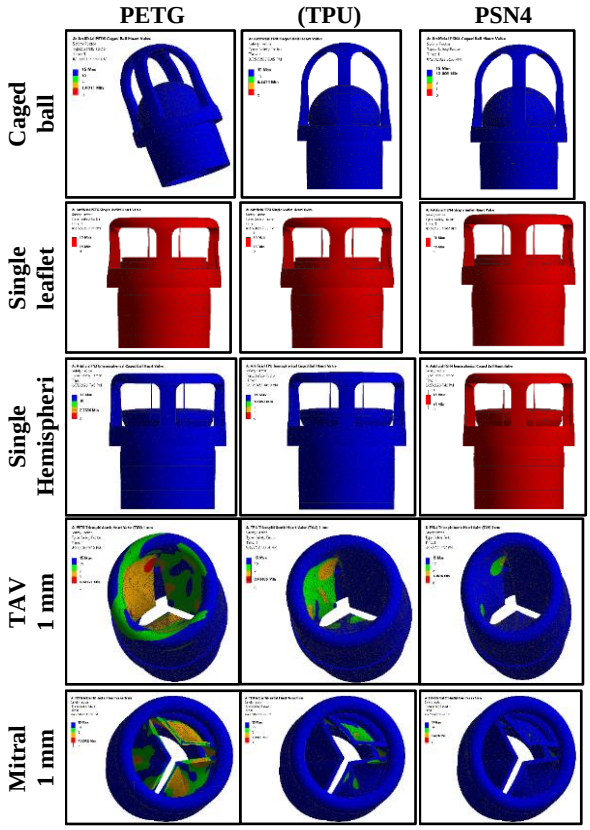

Figure 10. The stress safety factor simulations for selected types and the used materials of the designed artificial heart valves

Figure 13 shows the relationship between the produced heart valve type and the used material with the total deformation produced in the valve structure under the influence of applying the same blood pressure above. The figure shows that the highest total deformation in (mm), occurs when using thermoplastic polyurethane (TPU), followed by thermoplastic polyurethane

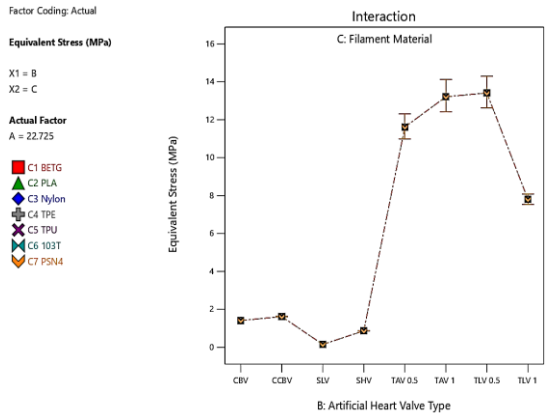

Figure 11. The equivalent stress for each produced artificial heart valve type

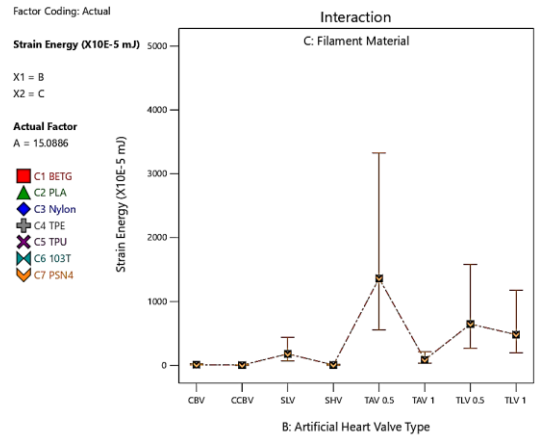

Figure 12. The expended strain energy for each designed artificial heart valve types

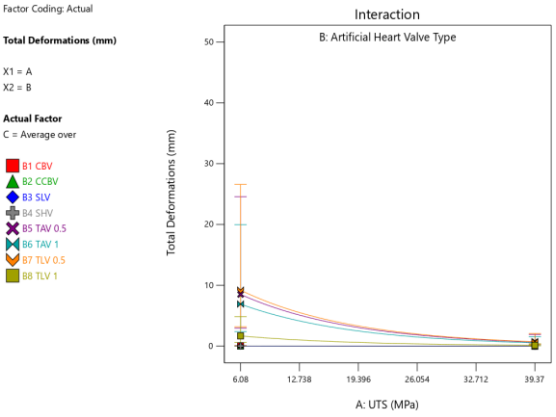

Figure 13. The total deformation produced in each artificial heart valve structure under the influence of applying the blood pressure

elastomer (TPE), nylon, polyethylene terephthalate glycol (PETG) and polyester PLA (Polylactic acid). Also, the lowest rates of deformation under the influence of blood pressure were observed when using materials of superior flexibility and strength, such as the used nanocomposite polyetherimide/silicone rubber with nano silica (PSN4), reaching from 5x10-5 to 0.1 mm, followed by the polystyrene- isobutylene-b-styrene (SIBSTAR103T) nanostructured rubber linear triblock.

Figure 14 shows the relationship between the material and type of the produced artificial heart valve with the stress safety factor, where the obtained values of this factor decrease with the complexity of the movement of the moving parts of the valve.

The highest rates were recorded when using the mitral tri-leaflet valve (tri-leaflet thick. = 1.0 mm) and reached 2.45 when using the high-strength and flexible PSN4 nanocomposite material. This value decreases to 1.27 when using the same material and type of valve but with a tri-leaflet thick. = 0.5 mm.

It is noted here that the PSN4 material is the only suitable for the manufacture of this artificial valve type, as well as the tricuspid aortic valve (TAV), where the other six tested materials failed because the stress safety factors are less than 1.

For the other types of manufactured valves, it was noted that the highest safety factor reached 15 was obtained when using the single-leaflet type valve, where all materials used in this work are suitable for the production of this type of valve because its movement is simple, flat, and in one direction. The principle of action of the tri-leaflet mechanical heart valve (BMHV) is that it has three semicircular leaflets prisms connected by small hinges with a solid, semi-circular valve ring instead of a single disc, and patients using this valve require anticoagulants for life (18). It has a much lower opening rate than the single-disc leaflet (33). It has a long service life and reliable performance and is of great importance in the treatment of valvular heart patients, but it still has defects such as thrombocytopenia, hemolysis, and thromboembolism (16, 20). The thickness of the leaflets is about 0.04D, and each leaflet can be opened up to 85

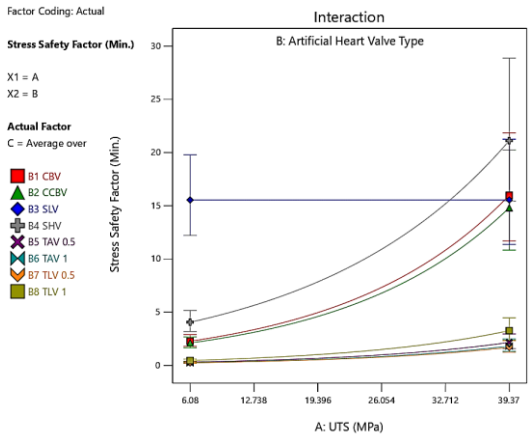

Figure 14. The stress safety factor for all the designed artificial heart valve types

degrees to obtain a rapid distribution of the flow velocity field of blood in the direction of the valve with less thrombosis (13, 21, 52).

The highest safety factor rates were observed after that when using the single hemispherical leaflet type valve, then the conical caged ball and the caged ball type, respectively. It can be concluded that the best materials for manufacturing these four types of valves are the PSN4, followed by the SIBSTAR103T, TPU, and TPE.

It is not recommended to use PETG, PLA, and nylon materials in the manufacture of any artificial heart valves, due to their lack of strength, flexibility, and high brittleness, especially PETG and PLA materials. SIBS material reinforced with woven polyester fabric or carbon nanotubes is also a promising material for the production of artificial heart valves. It has good mechanical properties, high thermal properties, and oxidative stability and is stable, biocompatible, and hematologically compatible making it an ideal candidate for medical applications (53, 54).

4. CONCLUSIONS

- It can be concluded that the best materials for manufacturing these four types of valves are the PSN4, followed by SIBSTAR103T, TPU, and TPE. The use of PETG, PLA, and nylon materials is not recommended in the manufacture of any prosthetic heart valves, due to their lack of strength, flexibility, and high brittleness, especially for PETG and PLA materials.
- It was also noted here that PSN4 is the only material suitable for the manufacture of mitral tri-leaflet and tricuspid mitral valve artificial valves. For other types of valves manufactured with a single leaflet, high safety stress factors were obtained because their movement is simple, flat, and in one direction, where the highest values were observed when testing a single hemispherical leaflet type valve, then the conical caged ball and the caged ball type, respectively .
- The highest values of the equivalent stress due to the applied blood pressure on the moving parts on each type of manufactured heart valve occur in valves with three dimensions moving parts, reached in the mitral tri-leaflet valve reached 14.13 MPa, followed by the tricuspid aortic valve. The equivalent stresses for other types of valves produced with simple surface action were lower than 2 MPa.
- The strain energy that is expended during the process of diastole and systole was found to be directly proportional to the strength and flexibility of the materials used. The energy consumption rates decrease when using highly elastic materials such as TPE and PSN4. The values of this energy also increase with an increase in the area of the moving parts of the valve, especially when faced with the process of closing blood flow, as with the use of the tricuspid aortic valve (TAV). The least values of energies were expended when using simple movement valves in one direction, including the single hemispherical leaflet, the caged ball, and then the single leaflet valves, respectively.
- The highest total deformation resulted in the valve body when using TPU, followed by TPE, nylon, PETG, and PLA, while the lowest deformation rates were observed when using PSN4, which ranged from 5x105 to 0.1 mm, followed by SIBSTAR103 nanostructured rubber.
- The obtained values of stress safety factors were decreased with the complexity of the movement for the moving parts of the valve. The highest rates were recorded when using the tricuspid mitral valve, reaching 2.45 when using the high-strength and flexible PSN4 nanomaterial .
- Additional future work is required to do mathematical modeling with numerical simulation of pressure distribution, blood flow velocity, and variable viscosity for all types of artificial heart valves presented in this paper.
- Working on the production of these types of artificial heart valves using the 3D bioprinting method, based on the successful application of tissue engineering in the development of heart valves to produce valves with mechanical properties similar to the original valves.

5. REFERENCES

1. Mitra M. Editorial on Advances in Artificial Heart. Ann Heart. 2018;3(1):51-2. 10.36959/652/390
2. Yoganathan AP, Fogel M, Gamble S, Morton M, Schmidt P, Secunda J, et al. A new paradigm for obtaining marketing approval for pediatric-sized prosthetic heart valves. The Journal of thoracic and cardiovascular surgery. 2013;146(4):879-86. 10.1016/j.jtcvs.2013.04.016
3. Ebad M, Vahidi B. In Silico Analysis of Stem Cells Mechanical Stimulations for Mechnoregulation Toward Cardiomyocytes. International Journal of Engineering, Transactions B: Applications, . 2022;35(11):2229-37. 10.5829/IJE.2022.35.11B.18
4. Hasan A, Soliman S, El Hajj F, Tseng Y-T, Yalcin HC, Marei HE. Fabrication and in vitro characterization of a tissue engineered PCL-PLLA heart valve. Scientific reports. 2018;8(1):8187. 10.1038/s41598-018-26452-y
5. Oveissi F, Naficy S, Lee A, Winlaw D, Dehghani F. Materials and manufacturing perspectives in engineering heart valves: a review. Materials Today Bio. 2020;5:100038. https://doi.org/10.1016/j.mtbio.2019.100038
6. Cook JA, Shah KB, Quader MA, Cooke RH, Kasirajan V, Rao KK, et al. The total artificial heart. Journal of thoracic disease. 2015;7(12):2172. 10.3978/j.issn.2072-1439.2015.10.70
7. Otto CM, Nishimura RA, Bonow RO, Carabello BA, Erwin III JP, Gentile F, et al. 2020 ACC/AHA guideline for the

management of patients with valvular heart disease: executive summary: a report of the American College of Cardiology/American Heart Association Joint Committee on Clinical Practice Guidelines. Journal of the American College of Cardiology. 2021;77(4):450-500. 10.1161/CIR.0000000000000932

8. Pibarot P, Dumesnil JG. Prosthetic heart valves: selection of the optimal prosthesis and long-term management. Circulation. 2009;119(7):1034-48. 10.1161/CIRCULATIONAHA.108.778886
9. Zhang DY, Lozier J, Chang R, Sachdev V, Chen MY, Audibert JL, et al. Case study and review: treatment of tricuspid prosthetic valve thrombosis. International journal of cardiology. 2012;162(1):14-9. 10.1016/j.ijcard.2011.09.081
10. Durko AP, Head SJ, Pibarot P, Atluri P, Bapat V, Cameron DE, et al. Characteristics of surgical prosthetic heart valves and problems around labeling: a document from the European Association for Cardio-Thoracic Surgery (EACTS)—the Society of Thoracic Surgeons (STS)—American Association for Thoracic Surgery (AATS) valve labelling task force. The Journal of thoracic and cardiovascular surgery. 2019;158(4):1041-54. 10.1093/ejcts/ezz034
11. Hasan A, Ragaert K, Swieszkowski W, Selimović Š, Paul A, Camci-Unal G, et al. Biomechanical properties of native and tissue engineered heart valve constructs. Journal of biomechanics. 2014;47(9):1949-63. https://doi.org/10.1016/j.jbiomech.2013.09.023
12. Ciolacu DE, Nicu R, Ciolacu F. Natural polymers in heart valve tissue engineering: Strategies, advances and challenges. Biomedicines. 2022;10(5):1095. https://doi.org/10.3390/biomedicines10051095
13. Rajashekar P. Development of mechanical heart valves-an inspiring tale. Journal of the Practice of Cardiovascular Sciences. 2015;1(3):289-93. 10.4103/2395-5414.177309
14. Rezvova MA, Klyshnikov KY, Gritskevich AA, Ovcharenko EA. Polymeric heart valves will displace mechanical and tissue heart valves: a new era for the medical devices. International Journal of Molecular Sciences. 2023;24(4):3963. https://doi.org/10.3390/ijms24043963
15. Gholami P, Kouchakzadeh MA, Farsi M. A continuum damage mechanics-based piecewise fatigue damage model for fatigue life prediction of fiber-reinforced laminated composites. International Journal of Engineering, Transactions C: Aspects. 2021;34(6):1512-22. 10.5829/IJE.2021.34.06C.15
16. Li W-q, Gao Z-x, Jin Z-j, Qian J-y. Transient study of flow and cavitation inside a bileaflet mechanical heart valve. Applied Sciences. 2020;10(7):2548. https://doi.org/10.3390/app10072548
17. Ghanbari J, Dehparvar A, Zakeri A. Design and analysis of prosthetic heart valves and assessing the effects of leaflet design on the mechanical attributes of the valves. Frontiers in Mechanical Engineering. 2022;8:764034. https://doi.org/10.3389/fmech.2022.764034
18. Nair K, Muraleedharan C, Bhuvaneshwar G. Developments in mechanical heart valve prosthesis. Sadhana. 2003;28:575-87. 10.1007/BF02706448
19. Dumont K. Experimental and numerical modeling of heart valve dynamics: Ghent University; 2004.
20. Dasi LP, Simon HA, Sucosky P, Yoganathan AP. Fluid mechanics of artificial heart valves. Clinical and experimental pharmacology and physiology. 2009;36(2):225-37. 10.1111/j.1440-1681.2008.05099.x
21. Jóźwik K, Witkowski D. Artificial heart valve designs. Mechanics and Mechanical Engineering. 2000;4(1):63--70.
22. Avinc O, Khoddami A. Overview of poly (lactic acid)(PLA) fibre: Part I: production, properties, performance, environmental impact, and end-use applications of poly (lactic acid) fibres. Fibre Chemistry. 2009;41(6):391-401. 10.1007/s10692-010-9213-z
23. Subbarao CV, Reddy YS, Inturi V, Reddy MI, editors. Dynamic mechanical analysis of 3D printed PETG material. IOP Conference Series: Materials Science and Engineering; 2021: IOP Publishing. 10.1088/1757-899X/1057/1/012031
24. Wang J, Yang B, Lin X, Gao L, Liu T, Lu Y, et al. Research of TPU materials for 3D printing aiming at non-pneumatic tires by FDM method. Polymers. 2020;12(11):2492. https://doi.org/10.3390/polym12112492
25. Storey RF, Baugh D, Choate K. Poly (styrene-b-isobutylene-b-styrene) block copolymers produced by living cationic polymerization: I. Compositional analysis. Polymer. 1999;40(11):3083-90. https://doi.org/10.1016/S0032-3861(98)00520-5
26. Pinchuk L, Wilson GJ, Barry JJ, Schoephoerster RT, Parel J-M, Kennedy JP. Medical applications of poly (styrene-block-isobutylene-block-styrene)("SIBS"). Biomaterials. 2008;29(4):448-60. https://doi.org/10.1016/j.biomaterials.2007.09.041
27. Mishra R, Rai J. Polyetherimide (PEI)/silicone rubber composite reinforced with nanosilica particles. International Journal of Scientific and Technology Research. 2016;5(3):176-80.
28. Nikoohemmat MA, Mazaheri H, Joshaghani A, Joudaki E. Investigation on Physical and Mechanical Properties of High Density Polyethylene (PE100) Using Novel Catalyst. International Journal of Engineering, Transactions B: Applications,. 2022;35(11):2205-12. 10.5829/IJE.2022.35.11B.15
29. Hirai S, Fukunaga S, Sueshiro M, Watari M, Sueda T, Matsuura Y. Assessment of a new silicone tri-leaflet valve seamlessly assembled with blood chamber for a low-cost ventricular assist device. Hiroshima journal of medical sciences. 1998;47(2):47-55.
30. Szykiedans K, Credo W, Osiński D. Selected mechanical properties of PETG 3-D prints. Procedia Engineering. 2017;177:455-61. https://doi.org/10.1016/j.proeng.2017.02.245
31. Wu Y, Gregorio R, Renzulli A, Onorati F, De Feo M, Grunkemeier G, et al. Mechanical heart valves: are two leaflets better than one? The Journal of thoracic and cardiovascular surgery. 2004;127(4):1171-9. 10.1016/j.jtcvs.2003.08.030
32. Harb SC, Rodriguez LL, Vukicevic M, Kapadia SR, Little SH. Three-dimensional printing applications in percutaneous structural heart interventions. Circulation: Cardiovascular Imaging. 2019;12(10):e009014. 10.1161/CIRCIMAGING.119.009014
33. Jin Y, Rao A, Brinkman W, Choi T-Y. 3D printing-assisted energy loss testing of artificial aortic heart valves. arXiv preprint arXiv:191011191. 2019. https://doi.org/10.48550/arXiv.1910.11191
34. Vukicevic M, Filippini S, Little SH. Patient-specific modeling for structural heart intervention: role of 3D printing today and tomorrow CME. Methodist DeBakey cardiovascular journal. 2020;16(2):130. 10.14797/mdcj-16-2-130
35. Altaani HA, Jaber S. Tricuspid valve replacement, mechnical vs. biological valve, which is better? International cardiovascular research journal. 2013;7(2):71.
36. C. S. Samuel and K. S. Candice. Bicuspid Aortic Valve Disease London and Toronto, Ontario, Canada. Journal of the American College of Cardiology,. 2010;55(25):2789–800. 10.1016/j.jacc.2009.12.068
37. Yousefi M, Safikhani H, Jabbari E, Tahmsbi V. Numerical modeling and optimization of respirational emergency drug delivery device using computational fluid dynamics and response surface method. International Journal of Engineering, Transactions B: Applications 2021;34(2):547-55. 10.5829/IJE.2021.34.02B.28

38. Karthik A, Kumar PP, Radhika T. A mathematical model for blood flow accounting for the hematological disorders. Computational and Mathematical Biophysics. 2022;10(1):184-98. https://doi.org/10.1515/cmb-2022-0136
39. Kabir MA, Sultana K, Uddin MA. Performance of k-ω and k-ε Model for Blood Flow Simulation in Stenosed Artery. Ganit: Journal of Bangladesh Mathematical Society. 2020;40(2). https://doi.org/10.3329/ganit.v40i2.51314
40. Kabir MA, Alam MF, Uddin MA. A numerical study on the effects of Reynolds number on blood flow with spiral velocity through regular arterial stenosis. Chiang Mai J Sci. 2018;45(6):2515-27.
41. Nanda S, Mallik BB, Majumder SD, Karthick RK, Suman S, Sonkar S. Mathematical Modelling of Pulsatile Flow of Non-Newtonian Fluid Through a Constricted Artery. Mathematical Modelling of Engineering Problems. 2021;8(3). https://doi.org/10.18280/mmep.080320
42. Owasit P, Sriyab S. Mathematical modeling of non-Newtonian fluid in arterial blood flow through various stenoses. Advances in Difference Equations. 2021;2021(1):1-20. https://doi.org/10.1186/s13662-021-03492-9
43. Nikolić A, Topalović M, Simić V, Blagojević M. BLOOD FLOW IN ARTERIAL BIFURCATION CALCULATED BY TURBULENT FINITE ELEMENT MODEL. Journal of the Serbian Society for Computational Mechanics/Vol. 2021;15(2):79-92. 10.24874/jsscm.2021.15.02.08
44. Labadin J, Ahmadi A, editors. Mathematical modeling of the arterial blood flow. Proceedings of the 2nd IMT-GT Regional Conference on Mathematics, Statistics and Applications, Universiti Sains Malaysia, Penang; 2006.
45. Rahman MS, Haque MA, editors. Mathematical modeling of blood flow. 2012 International Conference on Informatics, Electronics & Vision (ICIEV); 2012: IEEE. 10.1109/ICIEV.2012.6317446
46. Chakravarty S, Mandal P. Mathematical modelling of blood flow through an overlapping arterial stenosis. Mathematical and computer modelling. 1994;19(1):59-70.
47. Ali SM, Ali ZJ, Abd MM, editors. Design and Modeling of a Soft Artificial Heart by Using the SolidWorks and ANSYS. IOP Conference Series: Materials Science and Engineering; 2020: IOP Publishing. 10.1088/1757-899X/671/1/012062
48. Jalili P, Kazerani K, Jalili B, Ganji D. Investigation of thermal analysis and pressure drop in non-continuous helical baffle with different helix angles and hybrid nano-particles. Case Studies in Thermal Engineering. 2022;36:102209. https://doi.org/10.1016/j.csite.2022.102209
49. Rajaee M, Hosseinipour S, Jamshidi Aval H. Multi-objective optimization of HMGF process parameters for manufacturing AA6063 stepped tubes using FEM-RSM. International Journal of Engineering, Transactions B: Applications 2021;34(5):1305-12. 10.5829/IJE.2021.34.05B.25
50. Jalili P, Ganji D, Nourazar S. Investigation of convective-conductive heat transfer in geothermal system. Results in Physics. 2018;10:568-87. https://doi.org/10.1016/j.rinp.2018.06.047
51. Daebritz SH, Sachweh JrS, Hermanns B, Fausten B, Franke A, Groetzner J, et al. Introduction of a flexible polymeric heart valve prosthesis with special design for mitral position. Circulation. 2003;108(10_suppl_1):II-134-II-9. 10.1161/01.cir.0000087655.41288.dc
52. Khalili F, Gamage P, Mansy HA. Hemodynamics of a bileaflet mechanical heart valve with different levels of dysfunction. arXiv preprint arXiv:171111153. 2017. 10.15406/jabb.2017.02.00044
53. Makarevich MI, Nikishau PA, Berezianko IA, Glushkova TV, Rezvova MA, Ovcharenko EA, et al. Aspects of the synthesis of poly (styrene-block-isobutylene-block-styrene) by TiCl4-co-initiated cationic polymerization in open conditions. Macromol. 2021;1(4):243-55. https://doi.org/10.3390/macromol1040017
54. Farah S, Anderson DG, Langer R. Physical and mechanical properties of PLA, and their functions in widespread applications—A comprehensive review. Advanced drug delivery reviews. 2016;107:367-92. 10.1016/j.addr.2016.06.012

Persian Abstract

چکیده

جایگزینی دریچه قلب یک بار سلامتی بزرگ است و میلیون‌ها نفر در سراسر جهان به آن نیاز دارند، که نیاز مستمر به کشف و ساخت جایگزین‌های مصنوعی مؤثرتر و دائمی‌تر را می‌طلبد. در کار حاضر، مدل های منحصر به فرد هشت دریچه قلب مصنوعی با استفاده از هفت ماده مصنوعی و نانوکامپوزیت طراحی و مورد بررسی قرار گرفت. شیرهای طراحی شده برای تعیین بهترین طرح ها و مواد از نظر دوام، انعطاف پذیری، مصرف انرژی و عملکرد مورد بررسی قرار گرفتند. طراحی و شبیه سازی دریچه های مصنوعی انجام شد و برای اعتبارسنجی و بهبود عملکرد بیومکانیکی با استفاده از روش سطح پاسخ (RSM) و سیستم خبره طراحی ۱۳. بالاترین مقادیر تنش معادل به دلیل فشار خون اعمال شده بر روی قطعات متحرک در هر نوع دریچه قلب ساخته شده در دریچه هایی با قطعات متحرک سه بعدی که در دریچه سه لنگه میترال ۱٤.۱۳ مگاپاسکال و به دنبال آن دریچه آئورت سه لتی به دست می آید، رخ می دهد. تنش های معادل برای انواع دیگر شیرهای تولید شده با عملکرد سطحی ساده کمتر از ۲ مگاپاسکال بود. انرژی کرنشی که در طی فرآیند دیاستول و سیستول صرف می‌شود مشخص شد که با قدرت و انعطاف‌پذیری مواد مورد استفاده رابطه مستقیم دارد. نرخ مصرف انرژی هنگام استفاده از مواد بسیار الاستیک مانند TPE و PSN4 کاهش می یابد. مقادیر این انرژی نیز با افزایش سطح قسمت‌های متحرک دریچه افزایش می‌یابد، به‌ویژه هنگامی که با فرآیند بسته شدن جریان خون مواجه می‌شوید، مانند استفاده از دریچه آئورت سه لتی (TAV). بیشترین تغییر شکل کل در بدنه دریچه هنگام استفاده از TPU و به دنبال آن TPE، نایلون، PETG و PLA، در حالی که کمترین نرخ تغییر شکل در هنگام استفاده از PSN4 مشاهده شد که از x10۵ تا ۰.۱ میلی‌متر و به دنبال آن لاستیک نانوساختار SIBSTAR103 قرار داشت. مقادیر به‌دست‌آمده عوامل ایمنی تنش با پیچیدگی حرکت برای قسمت‌های متحرک شیر کاهش می‌یابد. بالاترین میزان در هنگام استفاده از دریچه میترال تریکوسپید ثبت شد و در هنگام استفاده از نانومواد PSN4 با مقاومت بالا و انعطاف پذیر به ۲.٤۵ رسید. می توان نتیجه گرفت که بهترین مواد برای ساخت این چهار نوع شیر، PSN4 و به دنبال آن SIBSTAR103T، TPU و TPE هستند. استفاده از مواد PETG، PLA و نایلون در ساخت هیچ گونه دریچه مصنوعی قلب به دلیل عدم استحکام، انعطاف پذیری و شکنندگی بالا به خصوص برای مواد PETG و PLA توصیه نمی شود. همچنین در اینجا ذکر شد که PSN4 تنها ماده مناسب برای ساخت دریچه های مصنوعی دریچه سه لفت و سه لتی میترال است. برای انواع دیگر دریچه‌های تولید شده با تک لت، فاکتورهای استرس ایمنی بالا به دست آمد زیرا حرکت آنها ساده، مسطح و در یک جهت است، جایی که بالاترین مقادیر را هنگام آزمایش یک دریچه از نوع منفرد نیم‌کره مشاهده شد، سپس توپ مخروطی در قفس مشاهده شد. و به ترتیب نوع توپ در قفس.